

A study on composite PtRu(1:1)-PtSn(3:1) anode catalyst for PEMFC

Dokyol Lee, Siwoo Hwang*, Insung Lee

Division of Materials Science and Engineering, Korea University, 5-1 Anam-Dong, Sungbuk-Ku, Seoul 136-701, South Korea

Accepted 14 February 2005
Available online 22 April 2005

Abstract

Composite PtRu(1:1)/C-PtSn(3:1)/C catalyst layers with various geometries and loadings were designed for a proton exchange membrane fuel cell (PEMFC) anode to improve carbon monoxide (CO) tolerance of the conventional PtRu(1:1)/C catalyst. The idea was based on an experimental finding that the onset potential of the PtSn for CO oxidation was lower than that of the PtRu and the resultant expectation that there seemed to be a possibility of using the PtSn as a CO filter. The CO tolerance of the composite catalyst of each design was judged by the cell performance obtained through a single cell test using H₂/CO gases of various CO concentrations and compared to that of the PtRu/C catalyst. The highest CO tolerance among the composite catalysts tested in this study was obtained for the one with geometry of double layers in the order of PtRu/C and PtSn/C from the electrolyte layer and with respective PtRu and PtSn loadings of 0.25 and 0.12 mg cm⁻². The cell with this composite catalyst showed better performance than the one with the PtRu/C catalyst. When a H₂/100 ppmCO gas was used as the fuel in the single cell test, the cell voltages were measured to be 0.49 and 0.44 V at a current density of 500 mA cm⁻², respectively for the cell with the composite and PtRu/C catalyst.

© 2005 Elsevier B.V. All rights reserved.

Keywords: Composite PtRu(1:1)/C-PtSn(3:1)/C catalyst; PEMFC; CO

1. Introduction

The proton exchange membrane fuel cells (PEMFCs) are operated at a relatively low temperature of about 80 °C. This low operating temperature makes PEMFCs very attractive especially in the field of mobile applications because it leads to rapid cell start-up. There still remain, however, some problems to be solved in the way to the commercialization of PEMFCs, and carbon monoxide (CO) poisoning of anode is one of them [1]. Basically hydrogen is used as a fuel for PEMFCs, but others such as natural gas and various hydrocarbons can also be used after reformed. The reformed fuels, however, generally contain carbon monoxide that is known to degrade anode performance through poisoning of the conventional Pt/C anode catalyst. Therefore researches have been made to enhance the CO tolerance of the PEMFC anode.

There are basically three methods available to mitigate CO poisoning in PEMFCs: (i) blending very low levels of

oxidant into the fuel gas flow [2,3], (ii) increasing an operating temperature [4], and (iii) developing new catalysts more tolerant towards CO than existing catalysts. Regarding the first method, when an oxidant is added to the fuel stream, the utilization of the fuel will certainly be decreased, and the safety problem should also be considered. Furthermore, the chemical oxidation of CO by O₂ catalyzed by Pt at the anode reduces the amount of Pt available for producing a current from the oxidation of hydrogen. The operation of high temperatures as the second method is not feasible due to membrane dehydration and using temperature to mitigate CO poisoning is currently not practical.

One successful idea in the development of CO tolerant catalysts was to add the second element, for example Ru, Sn or Mo, to pure Pt and thus produce Pt alloy catalysts [5,6]. Among many Pt alloy catalysts that have been considered for CO tolerance, PtRu alloys certainly are the most studied. And the PtRu(1:1)/C catalyst evidently shows high CO tolerance. The use of the PtRu/C as an oxidation catalyst for H₂ containing CO at the anode leads to a lowering of the CO oxidation potential compared with that of the Pt/C catalyst.

* Corresponding author. Tel.: +82 2 3290 3813; fax: +82 2 923 3584.
E-mail address: bedouin@korea.ac.kr (S. Hwang).

On the other hand, PtSn(3:1)/C, one of candidate catalysts for CO tolerance, has been reported that the onset potential of CO oxidation was shifted toward more negative side compared to that of the PtRu(1:1)/C [7,8]. It can thus be expected that there seems to be a possibility of using the PtSn/C as a CO filter.

In this work, composite PtRu(1:1)-PtSn(3:1)/C catalyst layers with various geometries and loadings were designed for a PEMFC anode to improve CO tolerance of the conventional PtRu(1:1) catalyst. The CO tolerance of the composite catalyst in the hydrogen oxidation reaction was evaluated through a single cell test using H₂/CO gases of various CO concentrations as the fuel and compared to that of the PtRu(1:1) catalyst.

2. Experimental

2.1. Preparation of Pt alloy catalysts and MEA's

20 wt.% M/C (M = PtRu(1:1) or PtSn(3:1)) catalysts were prepared using a colloidal method [9,10]. Tetraoctylammonium triethylhydroborate was used in the method as a reducing and stabilizing agent. The agent was added drop by drop at a rate of 2 cm³ min⁻¹ to a suspension solution of metal salt at 40 °C with the latter being stirred vigorously. The resulting colloidal solution was stirred for 4 h. A small amount of acetone was then added to the solution to remove excess reducing agent and stirring was continued for additional 1 h. For production of carbon-supported catalysts, the colloidal solution was mixed with a carbon (Cabot, Vulcan XC-72) suspension in THF and placed in a vacuum chamber at room temperature for evaporation of the solvent. The dried PtRu/C catalyst was then subjected to a heat treatment at 300 °C for 2 h in H₂ atmosphere for removal of a surfactant shell. For the PtSn/C catalyst, however, the heat treatment was done at a lower temperature of 210 °C due to its low melting point.

The catalyst inks for anode were prepared by dispersing catalysts and Nafion[®] solution (Aldrich, 5 wt.% solution) in butyl acetate (Aldrich) as a solvent [11]. The amount of Nafion[®] ionomer was fixed at 1 mg cm⁻² for a gas diffusion layer (SGL, GDL 10BB). Then catalyst layers were formed by brushing these inks on a GDL. Here, In the case of catalyst layers, two things were done in this study in order to optimize the function of the PtSn catalyst as a CO filter. Firstly, three types of the catalyst layers were made geometrically: one with a single layer of PtRu/C-PtSn/C mixture and the others with double layers in the order of PtRu/C and PtSn/C from the electrolyte layer and vice versa. In all the types, metal loadings, namely, both PtRu and PtSn loadings were fixed at 0.2 mg cm⁻². Secondly, loadings were varied in the range of 0.1–0.3 mg cm⁻² for PtRu and of 0.08–0.24 mg cm⁻² for PtSn with total Pt loading fixed at 0.26 mg cm⁻², the value for PtRu(1:1) with loading of 0.4 mg cm⁻², for proper comparisons of their CO tolerance. Also the geometry was fixed at

the one with double layers in the order of PtRu/C and PtSn/C from the electrolyte layer.

The commercial electrode from E-tek (Pt loading: 0.4 mg cm⁻²) was used as a cathode. The MEA with an active area of 5 cm² was fabricated by pressing a sandwich of the anode and the cathode with a layer of pretreated Nafion[®] 117 in the middle at 140 °C, 170 kg cm⁻² for 90 s.

2.2. Characterization of Pt alloy catalysts

The prepared PtRu/C or PtSn/C catalyst was characterized using X-ray diffractometry (XRD, Rigaku Geigerflex DMAX-IIA) to determine their phases and particle sizes, and high-resolution transmission electron microscopy (HRTEM, JEOL JEM-2010) to study their particle morphology.

2.3. Electrochemical measurement

The electrochemical properties of Pt/C(E-tek), PtRu(1:1)/C and PtSn(3:1) catalysts were investigated using CO stripping voltammetry. A three-electrode cell was used for the electrochemical tests. A SCE and a Pt pellet were used respectively as the reference electrode and the counter electrode. The tests were carried out in 0.5 M H₂SO₄ solution at a scan rate of 50 mV s⁻¹ in the range of -0.3 to 1 V. A CO gas was passed for 3 min through a bubbler located right below the working electrode in the electrolyte before the potential scan was started. All the electrochemical measurements were made using a potentiostat/galvanostat (EG&G 263A).

The single cell test was carried out at 80 °C under atmospheric pressure using O₂ as an oxidant and H₂ with 0, 10, 50 or 100 ppm CO as a fuel, to investigate the effect of CO on the cell performance. The fuel and the oxidant were passed through humidifiers respectively at 90 and at 85 °C for saturation with water and fed, respectively to anode and to cathode. The cell voltage was measured using an electronic loader (Deagil electronics, EL 200P).

3. Results and discussion

3.1. Characterization of PtRu(1:1)/C and PtSn(3:1)/C catalysts

The XRD pattern of the PtRu/C catalyst is shown in Fig. 1(a). A detailed analysis of the pattern revealed that the PtRu/C catalyst consisted of two phases, a face-centered cubic phase and an amorphous carbon phase. The amorphous carbon phase is identified by the broad peak centred at $2\theta = 25^\circ$. The face-centered cubic phase was identified as a Pt-Ru solid solution. The lattice parameter of the solid solution was estimated from the (2 2 0) peak at $2\theta \sim 69^\circ$ to be 3.880 Å. This value is very much similar to 3.884 Å obtained by Radmilovic et al. [12] for the PtRu(1:1) catalyst prepared by an impregnation method. Pearson [13] reported that the lattice parameters

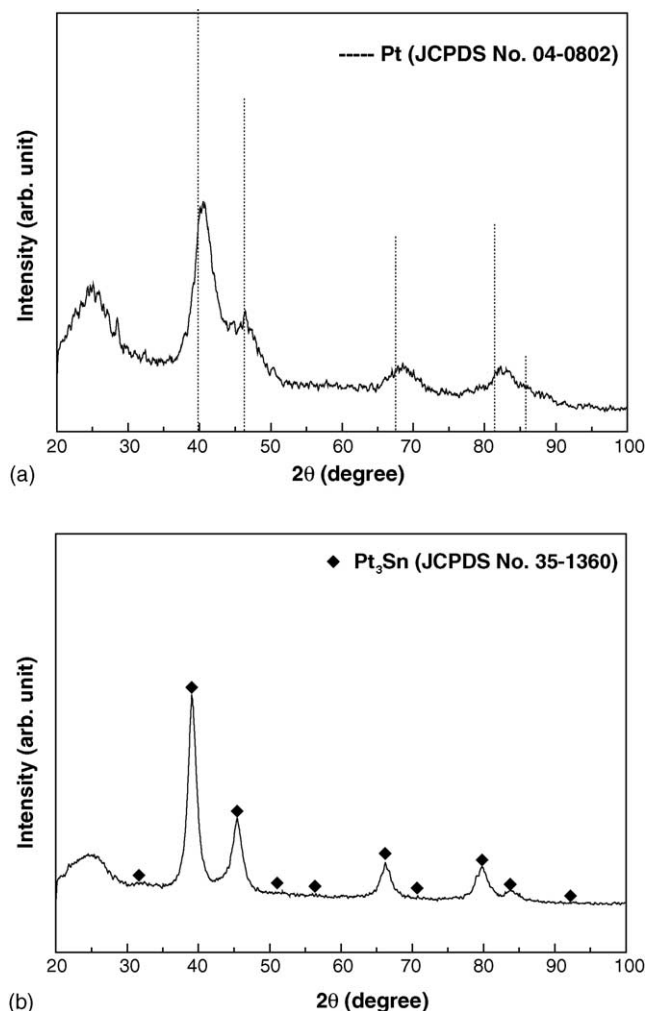


Fig. 1. XRD patterns of (a) PtRu(1:1)/C and (b) Pt₃Sn(3:1)/C catalysts prepared by a colloidal method.

of face-centered cubic PtRu bulk alloys decreased with increasing Ru content. With some of their lattice parameter data a calibration curve of lattice parameter versus Ru content was made assuming a linear relationship (Vegard's law). The Ru content in the PtRu catalyst could be estimated from the calibration curve as 46 at.%. This is close to 50 at.% for PtRu(1:1). The particle size of the PtRu catalyst was estimated also from the (2 2 0) peak using the Scherrer formula as 2.5 nm.

The XRD pattern of the PtSn/C catalyst is shown in Fig. 1(b). At a glance it looks similar to the pattern of the PtRu/C in (a). But the crystalline phase in (b) could not be identified as a face-centered Pt–Sn solid solution mainly because of a little peak at $2\theta \sim 32^\circ$. It is rather be a Pt₃Sn intermetallic compound. Pt₃Sn has a Cu₃Au structure with a simple cubic lattice and therefore, in addition to FCC sequential peaks of (1 1 1), (2 0 0), (2 2 0), (3 1 1) and (2 2 2), (1 0 0) and (1 1 0) peaks should appear in its XRD pattern. And the above-mentioned little peak turned out to be nothing but the (1 1 0) peak for Pt₃Sn. Also the crystalline peaks

are sharper in Fig. 1(b) than in Fig. 1(a), which means that the PtSn catalyst has larger particle size than the PtRu catalyst. Actually the particle size estimated for the PtSn catalyst shows much larger value of 5 than 2.5 nm for the PtRu catalyst. This seems to have been caused by the relatively high homologous temperature for heat treatment in the case of the PtSn catalyst.

Fig. 2 shows the HRTEM images of the PtRu/C and PtSn/C catalysts. It can be seen in the images that the particle size of PtRu/C is much smaller than that of PtSn/C which can be estimated roughly in (b) as 5 nm. This convinces us of the validity of the particle size values estimated from XRD patterns. It can also be seen in the images that the catalyst powders are distributed uniformly on carbon particles. The uniformity of catalyst powder distribution is known to be important for electrocatalytic activity.

3.2. CO stripping voltammetry

The electrocatalytic activity of the catalysts for CO oxidation was investigated using CO stripping voltammetry. The CO stripping voltammograms for the Pt/C (E-tek), PtRu/C and PtSn/C catalysts are shown in Fig. 3. The onset potential of CO oxidation for PtRu/C is observed in the figure to be lower by 0.25 V than that for Pt/C. This indicates that the electrocatalytic activity of PtRu/C is far superior to that of Pt/C. It is well known that the adsorption of oxygen-containing species like OH⁻ onto Ru commences at a potential as low as 0.2 V [14] which is compared to the value of 0.5 V for adsorption onto Pt. Hence, the superiority of the electrocatalytic activity of PtRu/C to that of Pt/C can be explained by the bifunctional mechanism for CO oxidation, that is, the removal of CO_{ads} proceeds via adsorbed OH_{ads} on Ru sites formed by dissociative water adsorption [4].

It can be seen also in Fig. 3 that the CO oxidation by PtSn/C commences at an even lower potential than the onset potential for PtRu/C. It appears that tin has the ability to promote the electro-oxidation of adsorbed CO at low potentials. Such an enhanced activity for CO oxidation may be interpreted as a contribution at lower potential due to electro-oxidation of weakly adsorbed CO on Pt₃Sn. The weakly adsorbed CO's seemed to cause the shift of the onset potential for PtSn/C toward the negative side with respect to that for PtRu/C. Gasteiger et al. [7] and Markovic et al. [8] have discussed the presence of strongly and weakly adsorbed CO's on a Pt single crystal surface and postulated creation of the weakly bonded CO adsorbed on Pt sites adjacent to Sn atoms in their Pt₃Sn alloy.

3.3. Performance of a single cell with Pt/C, PtRu/C or PtSn/C catalyst

Fig. 4 presents the cell voltage vs. current density characteristics of a single cell with the Pt/C, PtRu/C or PtSn/C catalyst. H₂, H₂/10 ppmCO, H₂/50 ppmCO or H₂/100 ppmCO gas was used as the fuel in the single cell test to see the effect

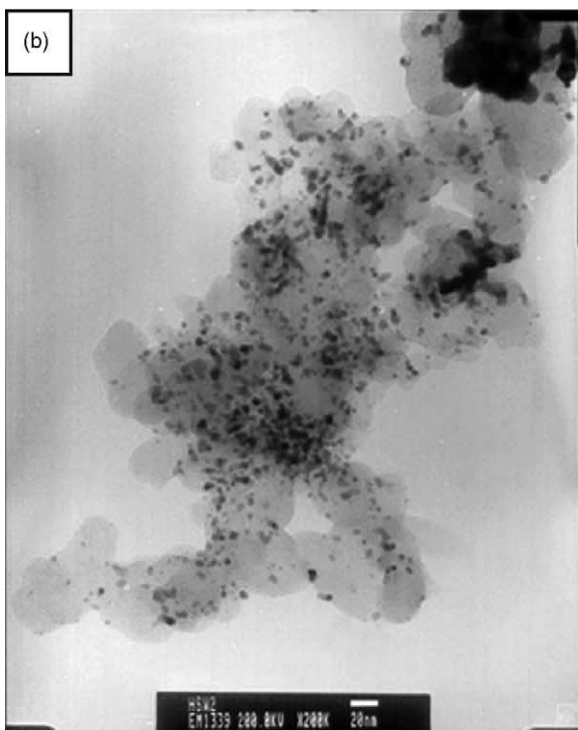
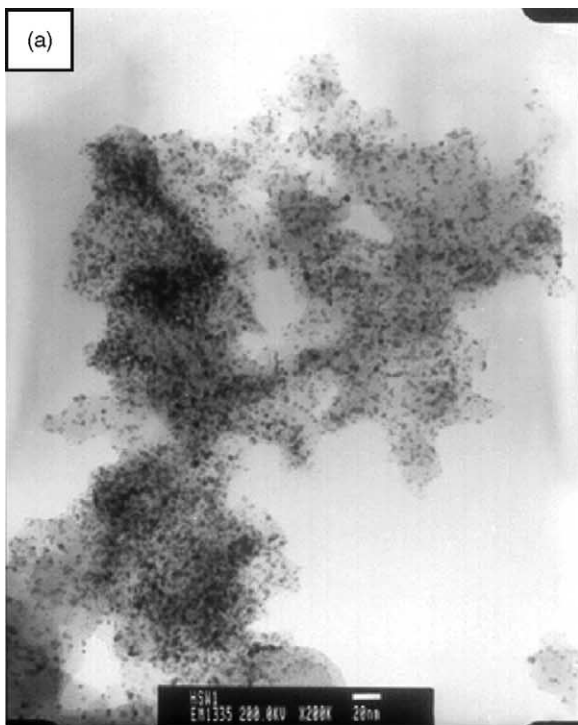


Fig. 2. TEM images ($\times 250,000$) of (a) PtRu(1:1)/C and (b) PtSn(3:1)/C catalysts prepared by a colloidal method.

of CO on polarization of anode and eventually on cell performance. In accordance with the characteristics obtained in other experimental investigations [15,16], the presence of CO in the fuel gas stream leads, regardless of the s of catalysts, to a marked decrease of cell performance with the amount of decrease increasing with increasing CO concentration. As

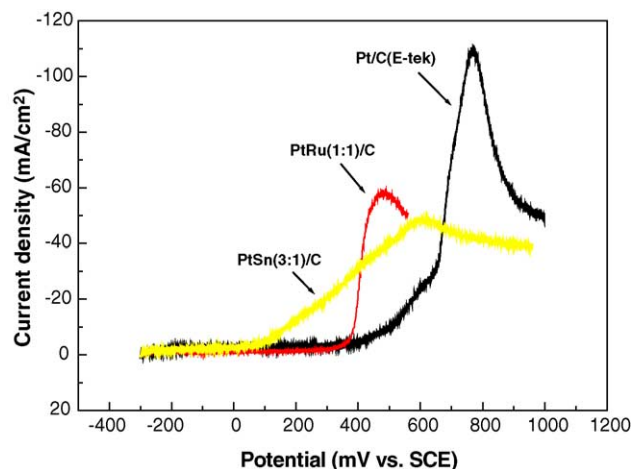


Fig. 3. CO stripping voltammograms for Pt/C, PtRu(1:1)/C and PtSn(3:1)/C catalysts obtained at 25 °C with a scan rate of 50 mV s⁻¹ in 0.5 M H₂SO₄ solution.

can be expected from the voltammograms in Fig. 3, the effect is maximal in the case of Pt/C catalyst. It can thus be said that the PtRu/C and PtSn/C catalysts showed higher CO tolerance than the Pt/C catalyst.

3.4. Performance of a single cell with a composite PtRu/C-PtSn/C catalyst

As mentioned above, three types were made in the geometry of the composite catalyst layers: one with a single layer of PtRu/C-PtSn/C mixture (type 1) and the others with double layers in the order of PtRu/C and PtSn/C from the electrolyte layer (type 2) and vice versa (type 3). The cell voltage versus current density curves for the three types are compared in Fig. 5 where CO concentration in the fuel gas was varied from 10 to 100 ppm. It can be seen clearly in the figure that even the two cells with a double-layer design show quite different performances depending on the order of catalyst layers. Thus, when the order from the electrolyte layer is PtRu/C-PtSn/C (type 2), the cell shows better performance than the one with a single layer (type 1) but the opposite is true when the order is the other way around. This can be justified by the fact that the PtSn catalyst plays the role of a CO filter more efficiently when the fuel gas stream passes through the PtSn layer prior to the PtRu layer than vice versa.

A single cell test was also carried out with the conventional PtRu(1:1) catalyst and the resultant performance data was compared to composite catalyst layers. Especially, in the atmosphere of H₂/100 ppmCO, type 2 shows practically similar performance within experimental errors up to a current density of 600 mA cm⁻² compared with the conventional PtRu(1:1) catalyst, but thereafter the former shows much better performance than the latter. This improvement in cell performance is thought to be due to higher CO tolerance of the former than that of the latter. The other cells with composite catalysts, however, did not show such improvement in cell performance. For this reason, we will fix the geometry

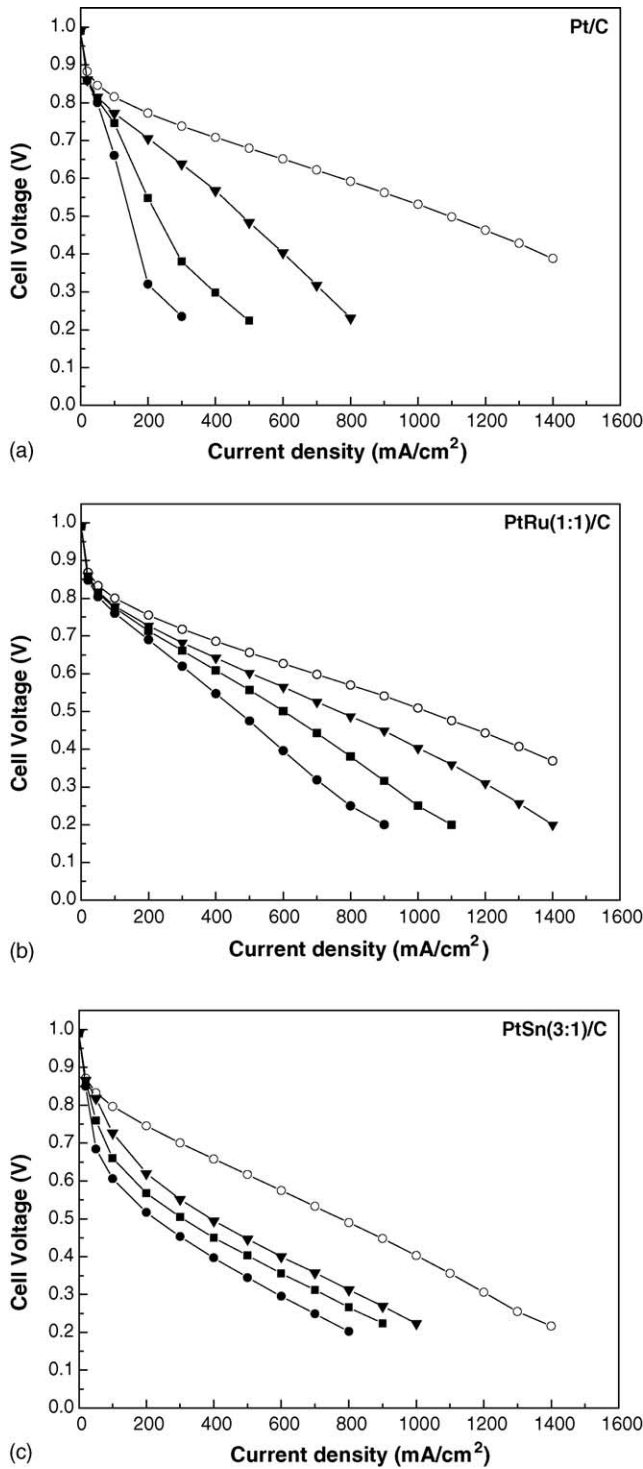


Fig. 4. The cell voltage vs. current density characteristics of a single cell with (a) Pt/C, (b) PtRu(1:1)/C and (c) PtSn(3:1)/C catalysts obtained at 80 °C using H₂ (○), H₂/10 ppmCO (▼), H₂/50 ppmCO (■) or H₂-100 ppmCO (●) as the fuel.

of composite catalyst layers at type 2 and focus only on the variation of PtRu and PtSn loadings hereafter. At first the variation of loadings was made only for PtSn but later for both.

Fig. 6 shows the change of relative cell voltage with time at a current density of 500 mA cm⁻² obtained for the cells with the PtRu/C and composite catalyst of 0.16, 0.20 and 0.40 mg cm⁻² PtSn loading using a H₂ gas with 10, 50

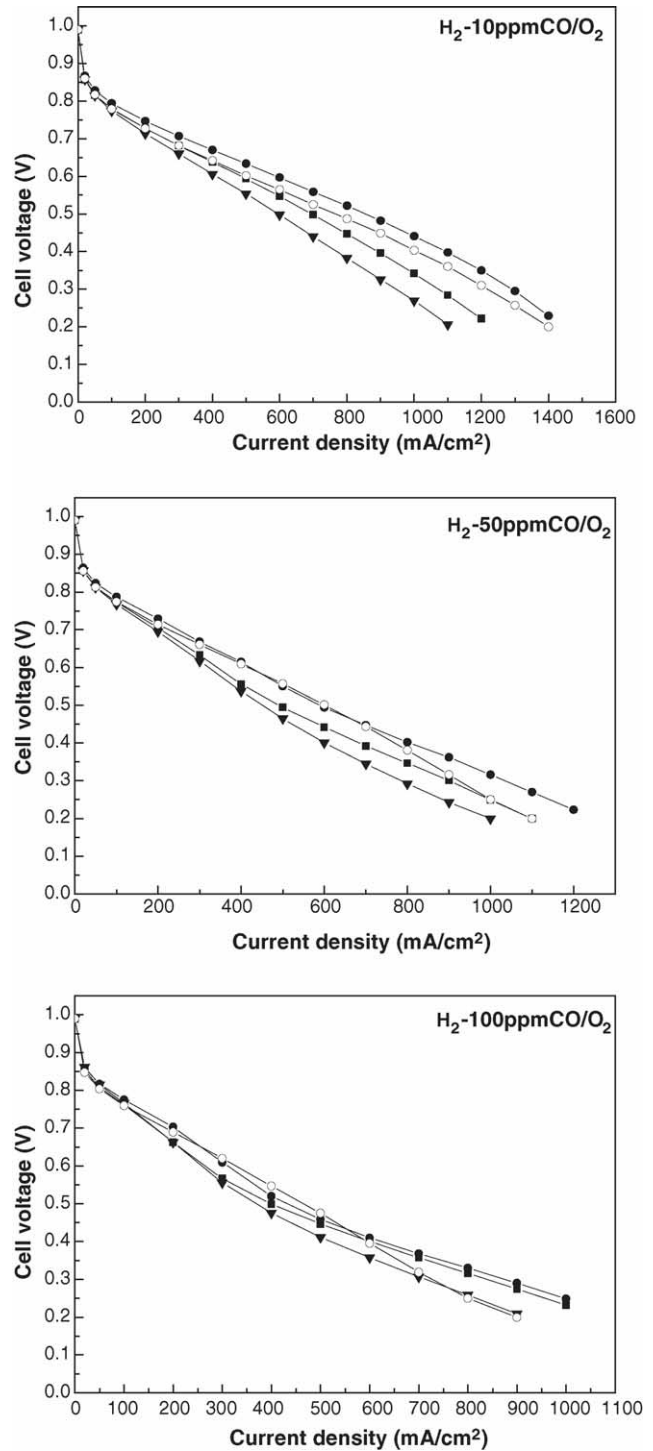


Fig. 5. The cell voltage vs. current density characteristics of the cells with three composite catalyst layer designs and PtRu(1:1)/C catalysts: (■) a single layer of a PtRu/C-PtSn/C mixture, (●) double layers in the order of PtRu/C and PtSn/C from electrolyte, (▼) double layers of the opposite order, and (○) a single layer of PtRu/C.

or 100 ppm CO as the fuel. Here, PtRu loading is fixed at 0.20 mg cm^{-2} . Compared to a cell with the PtRu catalyst, the cells with the composite catalyst show better performance no matter what PtSn loading is. And the cell performance

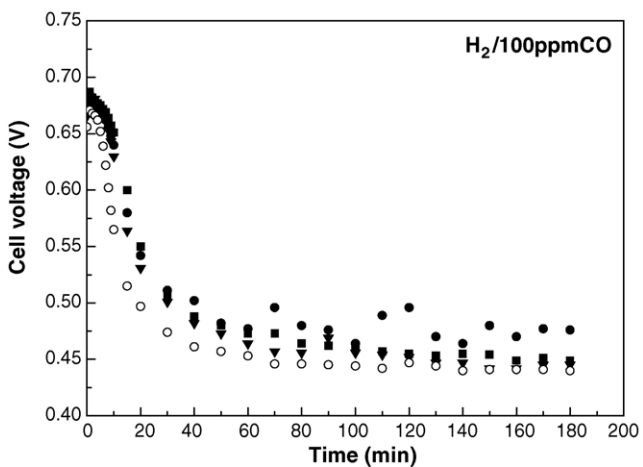
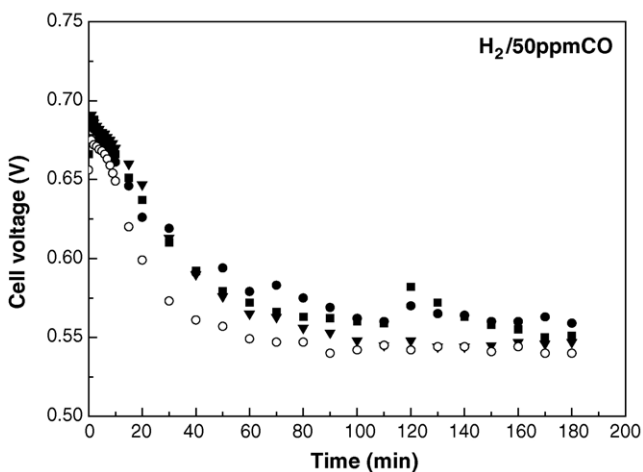
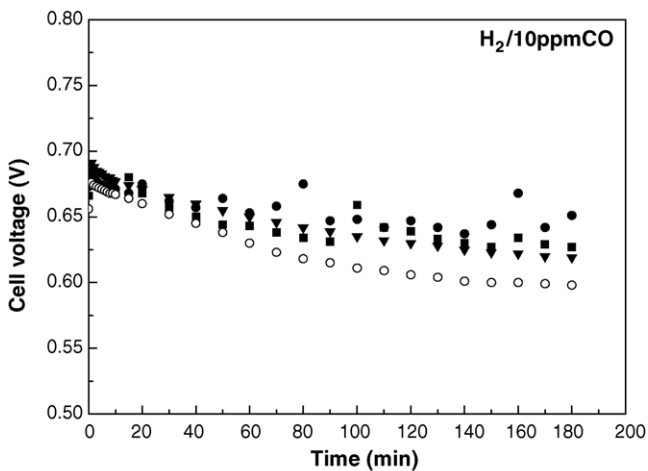


Fig. 6. The change of relative cell voltage with time at a current density of 500 mA cm^{-2} for the cells with the PtRu/C (\circ) and composite catalysts of PtSn/C loading of (∇) 0.16 mg cm^{-2} , (\blacksquare) 0.2 mg cm^{-2} and (\bullet) 0.4 mg cm^{-2} .

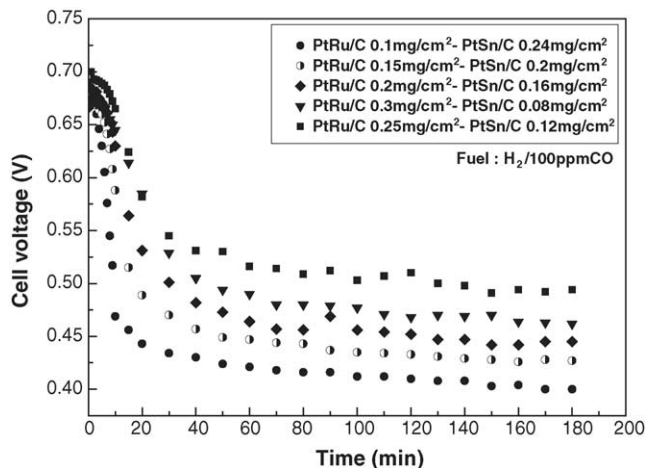


Fig. 7. The change of relative cell voltage with time at a current density of 500 mA cm^{-2} for the cells with composite catalyst of different PtRu/C and PtSn/C loadings. Here total Pt loading is fixed at 0.26 mg cm^{-2} .

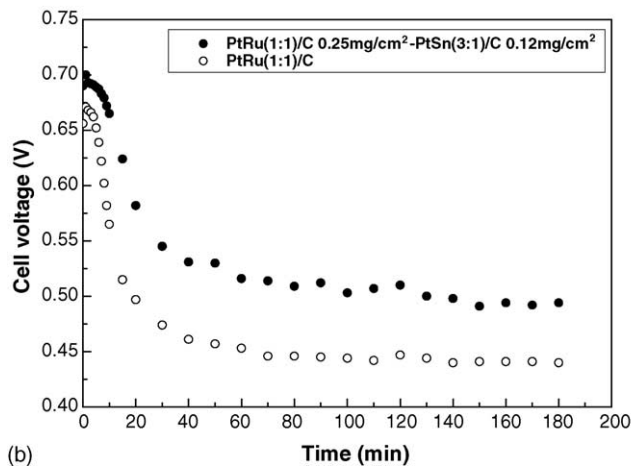
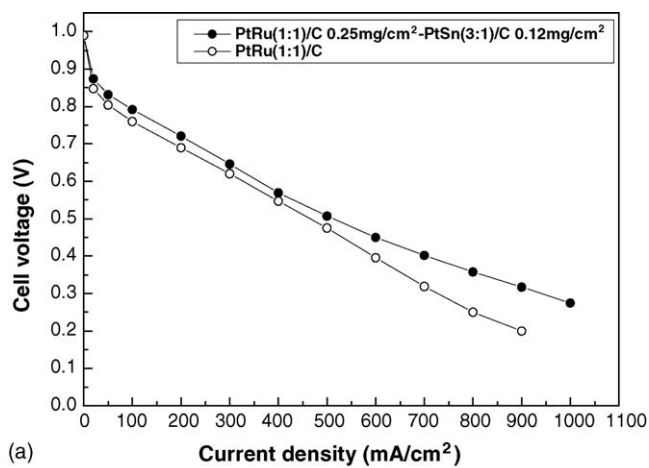


Fig. 8. Single cell performance plots obtained for the cells with the composite and PtRu/C catalysts using a H_2 -100 ppmCO/ O_2 gas as the fuel: (a) the cell voltage vs. current density characteristics and (b) the change of relative cell voltage with time at a current density of 500 mA cm^{-2} .

gets better as PtSn loading increases, which confirms that the PtSn catalyst is indeed playing the role of a CO filter and thus enhancing the CO tolerance. Based on the results in Fig. 6, it can be concluded that the cell performance is improved, when the composite PtRu/C-PtSn/C catalyst is used in place of the PtRu/C catalyst, with the extent of improvement proportional to PtSn loading.

Yet there is a possibility that the above conclusion may be wrong because the difference in cell performance observed in Fig. 6 might have resulted from the difference in total Pt loading rather than from the difference in PtSn loading. Therefore, in the following cell tests, PtRu and PtSn loadings were varied with the total Pt loading fixed at 0.26 mg cm^{-2} , the value for PtRu(1:1) with 0.4 mg cm^{-2} loading. Fig. 7 presents the change of relative cell voltage with time at a current density of 500 mA cm^{-2} obtained for the cells with the composite catalyst of different PtRu and PtSn loadings using a $\text{H}_2/100 \text{ ppmCO}$ gas as the fuel. According to the figure, the highest cell voltage or the best cell performance was obtained for the case with respective PtRu and PtSn loadings of 0.25 and 0.12 mg cm^{-2} . The cell voltage versus current density characteristics and the relative cell voltage versus time characteristics obtained for this cell using a $\text{H}_2/100 \text{ ppmCO}$ gas as the fuel are compared with the corresponding characteristics for the cell with the PtRu catalyst respectively in Fig. 8. It can be clearly seen in Fig. 8(a) that the cell with the composite catalyst shows better performance than the one with the PtRu/C catalyst. And the cell voltages, when stabilized, were measured in Fig. 8(b) to be 0.49 and 0.44 V at a current density of 500 mA cm^{-2} respectively for the cells with the composite and PtRu/C catalysts.

4. Conclusion

Composite PtRu(1:1)/C-PtSn(3:1)/C catalyst layers with various geometries and loadings were designed for a PEMFC anode to improve CO tolerance of the conventional PtRu(1:1)/C catalyst. The CO tolerance of the composite catalyst of each design was judged by the cell performance obtained through a single cell test using H_2/CO gases of various CO concentrations and compared to that of the PtRu/C catalyst and following conclusions can be made.

1. Three types were made in the geometry of the composite catalyst layers. When the order from the electrolyte layer is PtRu/C-PtSn/C, the cell shows better performance than the one with a single layer but the opposite is true when the order is the other way around.
2. Compared to a cell with the PtRu catalyst, the cells with the composite catalyst showed better performance no matter what PtSn loading is. And the cell performance gets better as PtSn loading increases, which confirms that the PtSn catalyst is indeed playing the role of a CO filter and thus enhancing the CO tolerance.
3. The highest cell voltage or the best cell performance was obtained for the case with respective PtRu and PtSn loadings of 0.25 and 0.12 mg cm^{-2} . When a $\text{H}_2/100 \text{ ppmCO}$ gas was used as the fuel in the single cell test, the cell voltages were measured to be 0.49 and 0.44 V at a current density of 500 mA cm^{-2} respectively for the cell with the composite and PtRu/C catalyst.

Acknowledgement

This work was supported by R01-2001-000-00045-0 from the Basic Research Program of the Korea Science and Engineering Foundation.

References

- [1] J. Divisek, H.F. Oetjen, V. Peinecke, V.M. Schmidt, U. Stimming, *Electrochim. Acta* 43 (1998) 3811.
- [2] S. Gottesfeld, J. Pafford, J. Electrochem. Soc. 135 (1988) 2651.
- [3] V.M. Schmidt, H.F. Oetjen, J. Divisek, J. Electrochem. Soc. 144 (1997) L237.
- [4] J.J. Baschuk, X. Li, *Int. J. Energy Res.* 25 (2001) 695.
- [5] S.J. Lee, S. Mukerjee, E.A. Ticianelli, J. McBreen, *Electrochim. Acta* 44 (1999) 3283.
- [6] S. Ball, A. Hodgkinson, G. Hoogers, S. Maniguet, D. Thompsett, B. Wong, *Electrochem. Solid State Lett.* 5 (2002) 31.
- [7] H.A. Gasteiger, N.M. Markovic, P.N. Ross Jr., *Catal. Lett.* 36 (1996) 1.
- [8] N.M. Markovic, B.N. Grgur, C.A. Lucas, P.N. Ross, *J. Phys. Chem. B* 103 (1999) 487.
- [9] T.J. Schmidt, M. Noeske, H.A. Gasteiger, R.J. Behm, P. Britz, H. Bönnemann, *J. Electrochem. Soc.* 145 (1998) 925.
- [10] T.J. Schmidt, M. Noeske, H.A. Gasteiger, R.J. Behm, P. Britz, W. Brijoux, H. Bönnemann, *Langmuir* 13 (1997) 2591.
- [11] M. Uchida, Y. Aoyama, N. Eda, A. Ohta, *J. Electrochem. Soc.* 142 (1995) 463.
- [12] V. Radmilovic, H.A. Gasteiger, P.N. Ross Jr., *J. Catal.* 154 (1995) 98.
- [13] W.B. Pearson, *A Handbook of Lattice Spacing and Structures of Metals and Alloys*, Pergamon, 1958, p. 823.
- [14] E. Tianelli, J.G. Beery, T. Paffett, S. Gottesfeld, *J. Electroanal. Chem.* 258 (1989) 61.
- [15] H.F. Oetjen, V.M. Schmidt, U. Stimming, F. Trilla, *J. Electrochem. Soc.* 143 (1996) 3836.
- [16] R.J. Bellows, E.P. Marucchi-Soos, D.T. Buckley, *Ind. Eng. Chem. Res.* 35 (1996) 1235.